

18 **Abstract:** Sedimentary records of lipid biomarkers such as leaf wax *n*-alkanes are not only
19 influenced by ecosystem turnover and physiological changes in plants, they are also influenced by
20 earth surface processes integrating these signals into the sedimentary record, though the effect of
21 these integration processes are not fully understood. To determine the depositional constraints on
22 biomarker records in a high-altitude small catchment system, we collected both soil and stream
23 sediments along a 1000 m altitude transect (1500 – 2500 masl) in the Areguni Mountains, a
24 subrange of the Lesser Caucasus Mountains in Armenia. We utilize a treeline at ~ 2000 masl,
25 which separates alpine meadow above from deciduous forest below, to assess the relative
26 contribution of upstream biomarker transport to local vegetation input in the stream. We find that
27 average chain length (ACL), hydrogen isotope (δD) and carbon isotope ($\delta^{13}C$) values of *n*-alkanes
28 are significantly different in soils collected above and below the treeline. However, samples
29 collected from the stream sediments do not integrate these signals quantitatively. As the stream drops
30 below the treeline, the ACL, δD and $\delta^{13}C$ values of *n*-alkanes preserved in streambed sediments
31 reflect a bias toward *n*-alkanes sourced from trees. This suggests that there is either 1) minimal
32 transportation of organic matter from the more open vegetation in higher elevations, or 2) greater
33 production of target biomarkers by trees and shrubs found at lower elevations results in
34 overprinting of stream signals by local vegetation. Though these observations may preclude using
35 *n*-alkanes to measure past treeline movement in these mountains, δD values of biomarkers in
36 fluvial deposits in these settings are more likely to record local hydrological changes rather than
37 reflect fractionation changes due to turnover in upstream vegetation structure.

38

39 **1. Introduction**

40 Mountain regions are important hubs for biodiversity and can provide refuge for a number
41 of endemic species of flora and fauna (Antonelli et al., 2018). However, these high-altitude
42 environments are often particularly vulnerable to climate change (Guisan and Theurillat, 2000).
43 Therefore, gaining an understanding of sensitivity of these regions to past climate change is
44 important for projecting the effects of future climate change on fragile ecosystems. The Caucasus
45 Region in particular has been identified as a biodiversity hotspot covering the Republics of
46 Armenia, Georgia, Azerbaijan, and parts of the Russian Federation, Türkiye, and Iran, that
47 supports a wide variety of plant and animal species (Zazanashvili, 2009; Gasparyan and
48 Glauberman, 2022). To better understand climate and environmental change in both the past and
49 the present, it is necessary to refine our understanding and interpretation of paleoclimate records
50 in this region. Plant wax biomarkers have been used in this region in both geological and
51 archaeological contexts to reconstruct past climates, therefore understanding modern variability
52 and transport processes will help refine these interpretations (Brittingham et al., 2019; Glauberman
53 et al., 2020; Malinsky-Buller et al., 2021, 2024; Trigui et al., 2019). Specifically, we are interested
54 in understanding the sedimentary processes involved in the formation, transport, recycling, and
55 accumulation of organic biomarkers in sedimentary archives and assessing whether these archives
56 record a local environmental signal or are a mix of local and transported organic material.

57 Normal alkanes (*n*-alkanes) are an important component of the epicuticular wax in
58 terrestrial plants. This waxy coating on plants protects against ultraviolet damage, water loss and
59 predation (Jetter et al., 2006). Specific compounds in this wax, such as *n*-alkanes, are a useful tool
60 for reconstructing past environmental changes through the analysis of the distribution of alkane
61 homologues as well as their stable hydrogen (δD) and carbon ($\delta^{13}C$) isotope values. Previous

62 research in the Greater and Lesser Caucasus Mountains has documented the applicability of the
63 average chain length (ACL) of leaf wax biomarkers as a tool for differentiating between grassy
64 and deciduous vegetation (Bliedtner et al., 2018; Trigui et al., 2019a), although on a global scale
65 ACL does not differentiate well between vegetation types (Bush and McInerney, 2013a).

66 The carbon isotope ($\delta^{13}\text{C}$) values of plant tissue is primarily determined by the
67 photosynthetic pathway of the plant (Diefendorf and Freimuth, 2017). C_3 plants, which thrive in
68 areas with cooler growing season temperatures, have more negative $\delta^{13}\text{C}$ values than do C_4 plants,
69 which thrive in warmer growing season temperatures (Ehleringer et al., 1977). C_3 vegetation is
70 further influenced by water use efficiency, as water stress influences the c_i/c_a ratio of plants
71 (Farquhar et al., 1982). $\delta^{13}\text{C}$ values in lipids generally follow the same trends, and C_3 plants have
72 more negative $\delta^{13}\text{C}$ lipid values than C_4 plants (Diefendorf and Freimuth, 2017). However, carbon
73 fractionation of lipids is not consistent in different classes of plants (Diefendorf et al., 2011;
74 Pedentchouk et al., 2008; Sikes et al., 2013). Currently, C_4 vegetation makes up around 3% of
75 plant species in Armenia (Rudov et al., 2020), and was present in the Kalavan region during the
76 Holocene (Tornero et al., 2016).

77 The hydrogen isotope (δD) values of *n*-alkanes in terrestrial plants record the δD values of
78 environmental water (Sachse et al., 2012). This is typically reflective of δD values in precipitation,
79 though precipitation δD values can also undergo positive shifts due to soil evaporation. The δD
80 values of plant waxes are also influenced by fractionation during biological synthesis of lipids,
81 which imparts a strong negative fractionation on δD values, as well as transpiration of leaf water
82 (Gamarra et al., 2016). The fractionation between meteoric water and lipids is typically larger in
83 gymnosperms than in angiosperms (Oakes and Hren, 2016; Pedentchouk et al., 2008).

84 Despite the benefits in measuring δD and $\delta^{13}\text{C}$ values in *n*-alkanes for understanding
85 environmental and hydrological processes, not all the processes modifying isotope values from
86 plant to *n*-alkane deposition are well understood. Sedimentary integration is one of the most poorly
87 understood aspects of this process (Sachse et al., 2012). A number of studies on the integration of
88 leaf waxes in catchments have been published in recent years which help clarify these processes
89 (Alewell et al., 2016; Feakins et al., 2018; Häggi et al., 2016; Hemingway et al., 2016; Ponton et
90 al., 2014; Suh et al., 2019). Previous studies on the integration of organic biomarkers have
91 produced mix results, with some demonstrating spatial integration of catchment signals (Alewell
92 et al., 2016; Feakins et al., 2018; Hemingway et al., 2016), whereas others did not observe this
93 (Häggi et al., 2016; Ponton et al., 2014). However, these previous studies typically focused on very
94 large river systems, which will undergo different transport processes than the first-order streams
95 analyzed in this study. A number of these studies (Alewell et al., 2016; Feakins et al., 2018;
96 Hemingway et al., 2016; Ponton et al., 2014) also observed seasonal differences in biomarker load
97 in river sediments.

98 Thus, the sedimentary processes involved in the formation, transport, recycling, and
99 accumulation of organic biomarkers in first and second order streams are not well understood. One
100 challenge in assessing these processes in small streams is that the environment and plant
101 communities are often homogenous, and thus it is not possible to differentiate between local and
102 upstream transported organic material. To better understand transport processes affecting organic
103 material in small catchments, we studied a set of streams in the Dany River, a tributary of the
104 Barepat River, located in the Areguni Mountains in the Lesser Caucasus Range. This stream
105 system is divided into two distinct ecological regions by the treeline (at ~ 2000 masl), which
106 separates alpine meadow above the tree line (2000 – 2500 masl) from deciduous forest below

107 (1500 – 2000 masl). To evaluate the input of *n*-alkanes from upstream transported organic material
108 relative to vegetation near the stream, we collected soil samples on the slopes of the mountains
109 from both above- and below the treeline throughout the watershed and sediments deposited in the
110 streambed along an elevation transect. Comparison of the hillside and streambed sedimentary *n*-
111 alkanes allows assessment of the input of *n*-alkanes locally produced by vegetation compared to
112 those transported in stream sediments within the catchment.

113 An additional motivation of this research is that treelines are a vulnerable feature of higher
114 altitude environments. Previous research in the Areguni Mountains study area has assessed the
115 relationship between treeline dynamics and climate forcing in the past (Ghukasyan et al., 2010;
116 Malinsky-Buller et al., 2021; Montoya et al., 2013; Tornero et al., 2016). Pleistocene sediments
117 uncovered at archaeological sites at Kalavan village within this area have the potential to
118 reconstruct this relationship through the analysis of plant wax biomarkers deposited in fluvial
119 sediments. However, in order to reconstruct these systems in the past it is important to understand
120 modern biomarkers integration processes in the first and second order streams and their potential
121 effects on the sedimentary archives of the Areguni Mountains.

122 **2. Methods**

123 **2.1 Sample Collection and Extraction**

124 Hillslope soil samples were collected in September 2018 along an altitude transect (1500 – 2500
125 masl) above the Dany River watershed, a first order tributary of the Barepat River in the Areguni
126 Mountains, Armenia (Fig 1), which traverses the treeline at ~2000 masl. Forest vegetation is
127 predominantly oak (*Quercus macranthera*), beech (*Fagus orientalis*) and hornbeam (*Carpinus*
128 *orientalis*), while above treeline alpine meadow is comprised of *Heracleum sp.* and *Senecio sp.*
129 (Joannin et al., 2022; Volodicheva, 2002). Soil samples were collected by first clearing the top ~10

130 cm of soil to remove roots. Stream bed sediment samples were collected from the Dany River
 131 throughout the altitude transect at intervals of ~100 m in altitude. In all cases, roughly 100 g of
 132 sediment were collected for extraction of *n*-alkanes. Samples were extracted using a Soxhlet
 133 apparatus with 2:1 dichloromethane:methanol for 48 hours. Following lipid extraction, *n*-alkanes
 134 were separated from total liquid extract by passing samples through a column of activated silica
 135 gel (1.25 g) in baked Pasteur pipettes with 2 mL hexane (non-polar fraction), 4 mL
 136 dichloromethane (slightly polar fraction) and 4 mL methanol (polar fraction). *n*-alkanes were
 137 quantified through the analysis of the hexane fraction. We quantified *n*-alkanes using a BP-5
 138 column (30 m × 0.25 mm i.d., 0.25 μm film thickness) with He as the carrier (1.5 ml/min). Oven
 139 temperature was set at 50 °C for 1 min, ramped to 180 °C at 12 °C/min, then ramped to 320 °C at
 140 6 °C/min and held for 4 min. (Brittingham et al., 2017; Smolen and Hren, 2023). We measured a
 141 standard mixture of *n*-alkanes (C₂₀-C₃₃) of known concentration to correct for mass dependent
 142 response decreases in longer chain *n*-alkanes. Odd over even predominance (OEP) (Eq. 1) and
 143 average chain length (ACL) (Eq. 2) were used to evaluate distributions of *n*-alkanes (Bush and
 144 McInerney, 2013b). We also calculated P_{aq}, an *n*-alkane proxy to evaluate the possible biomarker
 145 contribution of aquatic and emergent plants (Eq. 3) (Ficken et al., 2000).

$$146 \quad \text{OEP} = \frac{C_{25} + C_{27} + C_{29} + C_{31} + C_{33}}{C_{24} + C_{26} + C_{28} + C_{30} + C_{32}}$$

$$147 \quad \text{ACL} = \frac{25 * C_{25} + 27 * C_{27} + 29 * C_{29} + 31 * C_{31} + 33 * C_{33}}{C_{25} + C_{27} + C_{29} + C_{31} + C_{33}}$$

$$148 \quad \text{P}_{\text{aq}} = \frac{C_{23} + C_{25}}{C_{23} + C_{25} + C_{29} + C_{31}}$$

149 **2.3 Stable Isotope Analysis**

150 δD and $\delta^{13}\text{C}$ values of individual *n*-alkanes were measured with a Thermo GC-Isolink coupled
151 with a Thermo Scientific MAT 253 (manufacturer) isotope ratio mass spectrometer with a BP-5
152 column (30 m \times 0.25 mm i.d., 0.25 μm film thickness). Oven temperature was set at 50°C for 1
153 min, ramped to 180°C at 12°C/min, then ramped to 320°C at 6°C/min and held for 4 min. Internal
154 standards (Mix A5 from A. Schimmelman) were run every four samples across a range of
155 concentrations (5-30 V/s) to correct for size effects. Standard errors were 0.4‰ for $\delta^{13}\text{C}$ and 3‰
156 for δD . Isotope ratios (R) were converted to δX ($\delta^{13}\text{C}$ and δD) values (Eq. 3) and are expressed in
157 permill (‰).

$$158 \quad \delta\text{X} = \left(\frac{R_{\text{Sample}}}{R_{\text{Standard}}} - 1 \right) * 1000$$

159

160 **3. Results**

161 **3.1. Alkane abundances**

162 The most abundant alkane homolog in samples collected in the Areguni Mountains is the
163 C_{29} or C_{31} alkane, which is typical for terrestrial plants (see S1-S4 for illustrative chromatograms).
164 Odd numbered alkanes are significantly more abundant than even numbered alkanes, and the OEP
165 of all samples is 11.2, with a range from 7.4-18.4. There is no significant difference between the
166 mean OEP of soil (11.1) and stream (11.3) samples in the watershed. These values are similar to
167 those previously measured in the Greater and Lesser Caucasus Mountains (Bliedtner et al., 2018;
168 Trigui et al., 2019).

169 The mean average chain length (ACL) of all samples averages 29.7, with a range from 28.4
170 to 31.8 (Fig 3). In soils above the treeline, the mean ACL value is 30.6 (range of 29.8-31.8). In
171 soils below the treeline, the mean ACL value is 29.5 (range of 28.4-30.4). There is a significant

172 difference between the average ACL values of the *n*-alkanes in above treeline and below treeline
173 soils (Student's t-test, $p < 0.001$, $n = 30$). Stream sediment above the treeline have an average ACL
174 value of 29.7 (range of 29.1-30.2) and stream sediments below the treeline have an average ACL
175 value of 29.3 (range of 28.6 -30.0). The stream sediments from below the treeline have a
176 significantly (Student's t-test, $p < 0.001$, $n = 21$) lower average ACL value than those above the
177 treeline.

178 The P_{aq} values of *n*-alkanes in these samples suggests a mostly terrestrial origin of the
179 organic matter. Higher P_{aq} values indicate contributions of floating and emergent macrophytes.
180 However, we do not find a difference between the P_{aq} values in the stream sediments when
181 compared to the soil samples, indicating that the organic load of the stream sediments is mostly of
182 terrestrial origin. Terrestrial plants have average P_{aq} values of 0.09, with emergent plants averaging
183 0.25 (Ficken et al., 2000). Only eight of the 51 samples in this study had P_{aq} values above 0.20,
184 four stream and four soil samples. This indicates that there was not a significant contribution of
185 aquatic plants in the Dany stream sediments, and the biomarker load is primarily terrestrial in
186 origin.

187 **3.2. δD and $\delta^{13}C$ values**

188 The $\delta^{13}C$ values in soils and stream sediments collected from the Areguni Mountains reflect
189 a C_3 landscape, which is typical in Armenia. $\delta^{13}C$ values in all samples ranged from -36.0 to -
190 32.3‰ (Fig 4). The range is similar for both soil samples (-35.9 to -32.3‰) and stream samples (-
191 36.0 to -32.5‰). However, there is a significant difference in the $\delta^{13}C$ values of above and below
192 treeline samples, both in the stream and soil samples collected. Above the treeline, $\delta^{13}C$ values in
193 soils average -34.9‰, and below the treeline soil alkanes average -33.3‰ ($p < 0.0001$, student's t-
194 test, $n = 30$). Stream sediment $\delta^{13}C$ values average -35.0‰ above the treeline and -33.6‰ below

195 the treeline ($p < 0.0001$, student's t-test, $n=21$). $\delta^{13}\text{C}$ values in stream samples exhibit a step-like
196 behavior, with $\sim 2\text{‰}$ shift to more negative values as the stream drops below the treeline.

197 The δD values measured in soil samples collected in the catchment ranged from -144 to -
198 185‰ (Fig 5). These values were significantly more negative in above treeline sediments (-175‰)
199 than in below treeline sediments (-156‰) ($p < 0.001$, student's t-test, $n=30$). δD values were also
200 more negative in stream sediment samples collected above the treeline (-175‰) than below the
201 treeline (-158‰) ($p < 0.001$, student's t-test, $n=21$). As with the $\delta^{13}\text{C}$ values, the δD values of
202 stream sediment samples show sudden change as the stream drops below the treeline.

203 **4. Discussion**

204 **4.1 Integration of local and upstream soil *n*-alkanes into the river sediments**

205 The hillslope soil leaf wax ACL (Fig 3), $\delta^{13}\text{C}$ (Fig. 4) and δD (Fig. 5) show a step-like
206 change at the treeline, indicating a significant separation between upstream (above treeline) and
207 downstream (below treeline) soils. Using this separation, it is possible to assess the contributions
208 and integration of upstream vs. downstream soils to the streambed sediments along the altitude
209 transect. The step-like transition in streambed δD and $\delta^{13}\text{C}$ values indicates an over-printing of
210 upstream alkane isotope values by input from deciduous vegetation. Thus, local production largely
211 outweighs upstream transport in this setting. However, to firmly evaluate the upstream and
212 downstream hillslope soil contribution to streambed sediments, there is a need to quantitatively
213 evaluate the area-weighted production of *n*-alkanes above and below the treeline.

214 **4.2. Modeling *n*-alkane production and estimating upstream transport and integration**

215 To further evaluate the integration of *n*-alkanes above and below the treeline, we created a
216 mixing model that calculates the expected δD , $\delta^{13}\text{C}$ and ACL values at each one of the sampling
217 locations based on the *n*-alkane production of hillslope sediments above each streambed sampling

218 point (Fig. 6). Our mixing model assumes that the *n*-alkanes in the river are a function of the
219 weighted *n*-alkane production above the sampling location.

220 The parameters we used for our mixing model are: 1. Satellite images (Google Earth) to
221 map the areas covered by alpine meadow and forest vegetation throughout the Dany River
222 catchment. 2. An estimate of net primary productivity of organic material production in grasses
223 and trees (grams per area) (Brun et al., 2022). 3. Estimates of *n*-alkane production in grasses and
224 trees in the Greater and Lesser Caucasus Mountains (grams of *n*-alkane per gram of organic
225 material) (Bliedtner et al., 2018; Trigui et al., 2019). 4. End member values of δD , $\delta^{13}C$ and ACL
226 derived from the average hillslope soils above and below the treeline. At each sample point within
227 the catchment, we first calculated the upstream area covered by the two dominant vegetation types
228 within the catchment (deciduous forest and alpine meadow) (Figure 6). This area was then
229 multiplied by the previously mentioned constants (Table 1). By multiplying these terms (area x
230 organic mass production x *n*-alkane production x end member soils value), we created an *n*-alkane
231 production map for the Dany River catchment. Using this method, we calculated, the amount of
232 grass and tree *n*-alkanes produced on the hillslopes above the sampling locations and the expected
233 δD , $\delta^{13}C$ and ACL values for each stream sampling location (Figure 7a, 7c, 7e).

234 We compared the results of our mixing model with the measured δD , $\delta^{13}C$ and ACL in the
235 streams. Stream sediment samples collected above the treeline (from ~2000-2600 masl) fall within
236 the range of expected values, however, samples below the treeline consistently over-sample *n*-
237 alkanes sourced from below treeline vegetation. Measured δD , $\delta^{13}C$ and ACL values do not have
238 a linear relationship with the expected values based on vegetation area (Fig 7b, 7d, 7f). These
239 measured values would produce under-estimates of the upstream area of alpine grasses, yielding
240 incorrect reconstructions of paleo-vegetation in sedimentary records. Comparing the mixing model

241 with the observations indicates that an area-weighted mixing process is not an adequate model for
242 explaining the *n*-alkanes signal in the streambed sediments. A simple and straightforward way to
243 interpret this discrepancy is that an area-weighted quantitative integration of *n*-alkanes is not a
244 good model for describing this catchment system, and that local production is much larger than
245 transported organic material.

246 However, there are still other factors that may be driving this process that our mixing model
247 does not account for. First, the average slope of forested areas in the Dany watershed is higher than
248 those in grassy areas. These steeper slopes would cause more sediment transport into the stream
249 bed. Second, although production of *n*-alkanes in grasses and trees is not significantly different in
250 the Greater and Lesser Caucasus Mountains, concentrations are higher in soils in deciduous areas
251 (Bliedtner et al., 2018; Trigui et al., 2019). This retention of more biomarkers in forest soils would
252 also increase the contribution of deciduous alkanes into the stream bed. Third, stream downcutting
253 into older sediments has the potential to re-mobilize stored organic carbon, which may contain a
254 greater load of deciduous *n*-alkanes. However, analysis of pollen from a lake core nearby (~ 5km
255 from the Dany catchment) in the Areguni Mountains shows a gradual shift over the last 4000 years
256 from a grass-dominated landscape to the deciduous forest present today (Joannin et al., 2022b).
257 Therefore, stored biomarkers are more likely to be grass-dominant, and this is unlikely to explain
258 the measured bias to deciduous alkanes.

259 Since *n*-alkanes in the first order stream in this study do not quantitatively integrate *n*-alkanes
260 based on the upstream area of different vegetation types, this likely precludes the use of *n*-alkanes
261 as a tool to reconstruct vertical treeline movement in this setting. However, this is a benefit for
262 attempts to reconstruct hydrological changes through the analysis of δD values in *n*-alkanes. Given
263 the ~20‰ difference in apparent fractionation (ϵ) values for above and below treeline sediments,

264 changes in upstream vegetation cover would alter measured δD values in *n*-alkanes in sedimentary
265 archives. Without this quantitative integration, *n*-alkanes measured in the Pleistocene sediments
266 found in this watershed are more likely to reflect changes in δD values of precipitation, and
267 therefore would serve to reconstruct hydrological cycles, rather than changes in upstream
268 vegetation cover. Since $\delta^{13}C$ and ACL of *n*-alkanes are also different in above and below treeline
269 sediments, these other analyses would also be useful to identify periods with large changes in
270 treeline that might complicate interpretation of δD values.

271 In order to illustrate this point, we present hypothetical records of biomarker δD values
272 from three points in the Dany watershed (Fig. 7) documenting 20‰ and 30‰ shifts in precipitation
273 δD values. We use δD values of precipitation from water samples collected at the nearest
274 meteorological station with isotope data in Armenia (Dilijan, Brittingham et al., 2019b) Given the
275 lack of quantitative integration in the catchment, a paleoclimate record from either above (A) or
276 below (C) treeline would record the shift in precipitation δD values. Below treeline sedimentary
277 records, with stream organic biomarker load overprinted by local vegetation production, would
278 likely provide a means to reconstruct the δD precipitation values. However, records near the
279 treeline (B) would be influenced by changes in apparent fractionation values associated with
280 changes in vegetation around the stream. Co-occurring climate forcing of shifts in δD values of
281 precipitation and changes in treeline altitude would cause paleoclimate records in this zone to over-
282 estimate the magnitude of precipitation δD value shifts.

283

284 **5. Conclusion**

285 Sediment and stream samples from the Areguni Mountains, a subrange of the Lesser Caucasus
286 Mountains in Armenia, demonstrate that there is a significant difference in hillslope soil δD , $\delta^{13}C$

287 and ACL values above and below treeline. *n*-alkanes in sediments in the Areguni Mountains can
288 be used to differentiate between the above and below treeline sediments. However, *n*-alkanes
289 extracted from stream sediments reflect their local area, rather than demonstrating transport from
290 the higher-altitude alpine meadow. These results provide a complication for attempts to reconstruct
291 changes in past treeline in this mountain range, given that the biomarker load in stream does not
292 reflect the relative area of different upstream vegetation types. However, these results simplify
293 interpretation of past *n*-alkane δD values, as apparent fractionation differences between grasses
294 and trees are less likely to impart a significant influence on δD values in stream bed *n*-alkanes.

295 **6. Competing interests**

296 The contact author has declared that none of the authors has any competing interests

297 **7. Acknowledgements**

298 We would like to thank the Kalavan villagers for their help, support, and hospitality: especially
299 the Ghukasyan family for providing us a home away from home. We also thank Suren Kesejyan,
300 Hovhannes Partevyan, and Vardan Stepanyan. The research in Kalavan project was funded by the
301 support of The Gerda Henkel Stiftung grant n. AZ 10_V_17 and n. AZ 23/F/19, the Leakey
302 Foundation. AB is thankful to the Lady Davis foundation, Fritz-Thyssen Foundation grant awarded
303 for the project “Pleistocene Hunter-Gatherer Lifeways and Population Dynamics in the Ararat
304 (paleo-lake) Depression, Armenia”, and The European Research Council grant N 948015:
305 “Investigating Pleistocene population dynamics in the Southern Caucasus” (awarded to AMB) for
306 current financial support. Further support was provided by “Areni-1 Cave” Consortium [“Areni-1
307 Cave” Scientific-Research Foundation (Armenia), and the “Gfoeller Renaissance Foundation”
308 (USA)], as well as the Institute of Archaeology and Ethnography of the National Academy of
309 Sciences of the Republic of Armenia (supported by the Higher Education and Science Committee,

310 Republic of Armenia, under grant number 21AG-6A080). We would like to thank Joseph Novak
311 and an anonymous reviewer for their helpful comments on the manuscript.

312

313 **References**

314

315 Alewell, C., Birkholz, A., Meusburger, K., Schindler Wildhaber, Y., and Mabit, L.: Quantitative
316 sediment source attribution with compound-specific isotope analysis in a C3 plant-
317 dominated catchment (central Switzerland), *Biogeosciences*, 13, 1587–1596,
318 <https://doi.org/10.5194/bg-13-1587-2016>, 2016.

319

320 Antonelli, A., Kissling, W. D., Flantua, S. G. A., Bermúdez, M. A., Mulch, A., Muellner-Riehl,
321 A. N., Kreft, H., Linder, H. P., Badgley, C., Fjeldså, J., Fritz, S. A., Rahbek, C., Herman,
322 F., Hooghiemstra, H., and Hoorn, C.: Geological and climatic influences on mountain
323 biodiversity, *Nat Geosci*, 11, 718–725, <https://doi.org/10.1038/s41561-018-0236-z>, 2018.

324

325 Bliedtner, M., Schäfer, I. K., Zech, R., and Von Suchodoletz, H.: Leaf wax n-alkanes in modern
326 plants and topsoils from eastern Georgia (Caucasus) - Implications for reconstructing
327 regional paleovegetation, *Biogeosciences*, 15, 3927–3936, [https://doi.org/10.5194/bg-15-](https://doi.org/10.5194/bg-15-3927-2018)
328 [3927-2018](https://doi.org/10.5194/bg-15-3927-2018), 2018.

329

330 Brittingham, A., Hren, M., and Hartman, G.: Microbial alteration of the hydrogen and carbon
331 isotopic composition of n-alkanes in sediments, *Org Geochem*, 107, 1–8,
332 <https://doi.org/10.1016/j.orggeochem.2017.01.010>, 2017.

333

334 Brittingham, A., Hren, M. T., Hartman, G., Wilkinson, K. N., Mallol, C., Gasparyan, B., and
335 Adler, D. S.: Geochemical Evidence for the Control of Fire by Middle Palaeolithic
336 Hominins, *Sci Rep*, 9, <https://doi.org/10.1038/s41598-019-51433-0>, 2019a.

337

338 Brittingham, A., Petrosyan, Z., Hepburn, J. C., Richards, M. P., Hren, M. T., and Hartman, G.:
339 Influence of the North Atlantic Oscillation on δD and $\delta^{18}O$ in meteoric water in the
340 Armenian Highland, *J Hydrol (Amst)*, 575, 513–522,
341 <https://doi.org/10.1016/j.jhydrol.2019.05.064>, 2019b.

342

343 Brun, P., Zimmermann, N. E., Hari, C., Pellissier, L., and Karger, D. N.: Global climate-related
344 predictors at kilometer resolution for the past and future, *Earth Syst Sci Data*, 14, 5573–
345 5603, <https://doi.org/10.5194/essd-14-5573-2022>, 2022.

346

347 Bush, R. T. and McInerney, F. A.: Leaf wax n-alkane distributions in and across modern plants:
348 Implications for paleoecology and chemotaxonomy, *Geochim Cosmochim Acta*, 117,
349 161–179, <https://doi.org/10.1016/j.gca.2013.04.016>, 2013.

350

351

352 Diefendorf, A. F. and Freimuth, E. J.: Extracting the most from terrestrial plant-derived n-alkyl
353 lipids and their carbon isotopes from the sedimentary record: A review, *Org Geochem*,
354 103, 1–21, <https://doi.org/10.1016/j.future.2015.08.005>, 2017.
355

356 Diefendorf, A. F., Freeman, K. H., Wing, S. L., and Graham, H. V.: Production of n-alkyl lipids
357 in living plants and implications for the geologic past, *Geochim Cosmochim Acta*, 75,
358 7472–7485, <https://doi.org/10.1016/j.gca.2011.09.028>, 2011.
359

360 Ehleringer, J., Björkman, O., and Bjorkman, O.: Quantum yields for CO₂ uptake in C₃ and C₄
361 plants, *Plant Physiol*, 59, 86–90, 1977.
362

363 Farquhar, G. D., O’Leary, M. H., and Berry, J. A.: On the Relationship between Carbon Isotope
364 Discrimination and the Intercellular Carbon Dioxide Concentration in Leaves, *Aust J*
365 *Plant Physiol*, 9, 121–137, 1982.
366

367 Feakins, S. J., Wu, M. S., Ponton, C., Galy, V., and West, A. J.: Dual isotope evidence for
368 sedimentary integration of plant wax biomarkers across an Andes-Amazon elevation
369 transect, *Geochim Cosmochim Acta*, 242, 64–81,
370 <https://doi.org/10.1016/j.gca.2018.09.007>, 2018a.
371

372 Ficken, K. J., Li, B., Swain, D. L., and Eglinton, G.: An n -alkane proxy for the sedimentary
373 input of submerged floating freshwater aquatic macrophytes, *Org Geochem*, 31, 745–749,
374 2000.
375

376 Gamarra, B., Sachse, D., and Kahmen, A.: Effects of leaf water evaporative 2H-enrichment and
377 biosynthetic fractionation on leaf wax n-alkane $\delta^2\text{H}$ values in C₃ and C₄ grasses, *Plant*
378 *Cell Environ*, 39, 2390–2403, <https://doi.org/10.1111/pce.12789>, 2016.
379

380 Ghukasyan, R., Colonge, D., Nahapetyan, S., Ollivier, V., Gasparyan, B., Monchot, H., and
381 Chataigner, C.: Kalavan-2 (North of Lake Sevan, Armenia): A new late middle
382 paleolithic site in the Lesser Caucasus, *Archaeology, Ethnology and Anthropology of*
383 *Eurasia*, 38, 39–51, <https://doi.org/10.1016/j.aeae.2011.02.003>, 2010.
384

385 Glauberman, P., Gasparyan, B., Sherriff, J., Wilkinson, K., Li, B., Knul, M., Brittingham, A.,
386 Hren, M. T., Arakelyan, D., Nahapetyan, S., Raczynski-henk, Y., Haydosyan, H., and
387 Adler, D. S.: Barozh 12 : Formation processes of a late Middle Paleolithic open-air site in
388 western Armenia, *Quat Sci Rev*, 236, 106276, 2020.
389

390 Guisan, A. and Theurillat, J.-P.: Assessing alpine plant vulnerability to climate change: a
391 modeling perspective., *Integrated Assessment*, 307–320, 2000.
392

393 Häggi, C., Sawakuchi, A. O., Chiessi, C. M., Mulitza, S., Mollenhauer, G., Sawakuchi, H. O.,
394 Baker, P. A., Zabel, M., and Schefuß, E.: Origin, transport and deposition of leaf-wax

395 biomarkers in the Amazon Basin and the adjacent Atlantic, *Geochim Cosmochim Acta*,
396 192, 149–165, <https://doi.org/10.1016/j.gca.2016.07.002>, 2016a.
397

398 Hemingway, J. D., Schefuß, E., Dinga, B. J., Pryer, H., and Galy, V. V.: Multiple plant-wax
399 compounds record differential sources and ecosystem structure in large river catchments,
400 *Geochim Cosmochim Acta*, 184, 20–40, <https://doi.org/10.1016/j.gca.2016.04.003>, 2016.
401

402 Jetter, R., Kunst, L., and Samuels, A. L.: Composition of plant cuticular waxes, in: *Biology of*
403 *the Plant Cuticle*, edited by: Riederer, M. and Miller, C., Blackwell Publishing Ltd,
404 Oxford, 145–181, 2006.
405

406 Joannin, S., Capit, A., Ollivier, V., Bellier, O., Brossier, B., Mourier, B., Tozalakian, P.,
407 Colombié, C., Yevadian, M., Karakhanyan, A., Gasparyan, B., Malinsky-Buller, A.,
408 Chataigner, C., and Perello, B.: First pollen record from the Late Holocene forest
409 environment in the Lesser Caucasus, *Rev Palaeobot Palynol*, 304,
410 <https://doi.org/10.1016/j.revpalbo.2022.104713>, 2022a.
411

412 Malinsky-Buller, A., Glauberman, P., Ollivier, V., Lauer, T., Timms, R., Frahm, E., Brittingham,
413 A., Triller, B., Kindler, L., Knul, M. V., Krakovsky, M., Joannin, S., Hren, M. T., Bellier,
414 O., Clark, A. A., Blockley, S. P. E., Arakelyan, D., Marreiros, J., Paixaco, E., Calandra,
415 I., Ghukasyan, R., Nora, D., Nir, N., Adigoyalyan, A., Haydosyan, H., and Gasparyan,
416 B.: Short-Term occupations at high elevation during the Middle Paleolithic at Kalavan 2
417 (Republic of Armenia), *PLoS One*, 16, <https://doi.org/10.1371/journal.pone.0245700>,
418 2021.
419

420 Malinsky-Buller, A., Edeltin, L., Ollivier, V., Joannin, S., Peyron, O., Lauer, T., Frahm, E.,
421 Brittingham, A., Hren, M. T., Sirdeys, N., Glauberman, P., Adigoyalyan, A., and
422 Gasparyan, B.: The environmental and cultural background for the reoccupation of the
423 Armenian Highlands after the Last Glacial Maximum: The contribution of Kalavan 6, *J*
424 *Archaeol Sci Rep*, 56, <https://doi.org/10.1016/j.jasrep.2024.104540>, 2024.
425

426 Montoya, C., Balasescu, A., Joannin, S., Ollivier, V., Liagre, J., Nahapetyan, S., Ghukasyan, R.,
427 Colonge, D., Gasparyan, B., and Chataigner, C.: The Upper Palaeolithic site of Kalavan 1
428 (Armenia): An Epigravettian settlement in the Lesser Caucasus, *J Hum Evol*, 65, 621–
429 640, <https://doi.org/10.1016/j.jhevol.2013.07.011>, 2013.
430

431 Oakes, A. M. and Hren, M. T.: Temporal variations in the δD of leaf n-alkanes from four riparian
432 plant species, *Org Geochem*, 97, 122–130,
433 <https://doi.org/10.1016/j.orggeochem.2016.03.010>, 2016.
434

435 Pedentchouk, N., Sumner, W., Tipple, B., and Pagani, M.: $\delta^{13}C$ and δD compositions of n-
436 alkanes from modern angiosperms and conifers: An experimental set up in central

437 Washington State, USA, *Org Geochem*, 39, 1066–1071,
438 <https://doi.org/10.1016/j.orggeochem.2008.02.005>, 2008.

439

440 Ponton, C., West, A. J., Feakins, S. J., and Galy, V.: Leaf wax biomarkers in transit record river
441 catchment composition, *Geophys Res Lett*, 41, 6420–6427,
442 <https://doi.org/10.1002/2014GL061184>. Received, 2014.

443

444 Rudov, A., Mashkour, M., Djamali, M., and Akhiani, H.: A Review of C4 Plants in Southwest
445 Asia: An Ecological, Geographical and Taxonomical Analysis of a Region With High
446 Diversity of C4 Eudicots, *Front Plant Sci*, 11, <https://doi.org/10.3389/fpls.2020.546518>,
447 2020.

448

449 Sachse, D., Billault, I., Bowen, G. J., Chikaraishi, Y., Dawson, T. E., Feakins, S. J., Freeman, K.
450 H., Magill, C. R., McInerney, F. a., van der Meer, M. T. J. J., Polissar, P., Robins, R. J.,
451 Sachs, J. P., Schmidt, H.-L., Sessions, A. L., White, J. W. C., West, J. B., and Kahmen,
452 A.: Molecular paleohydrology: interpreting the hydrogen-isotopic composition of lipid
453 biomarkers from photosynthesizing organisms, *Annu Rev Earth Planet Sci*, 40, 221–249,
454 <https://doi.org/10.1146/annurev-earth-042711-105535>, 2012.

455

456 Sikes, E. L., Medeiros, P. M., Augustinus, P., Wilmshurst, J. M., and Freeman, K. R.: Seasonal
457 variations in aridity and temperature characterize changing climate during the last
458 deglaciation in New Zealand, *Quat Sci Rev*, 74, 245–256,
459 <https://doi.org/10.1016/j.quascirev.2013.01.031>, 2013.

460

461 Smolen, J. D. and Hren, M. T.: Differential effects of clay mineralogy on thermal maturation of
462 sedimentary n-alkanes, *Chem Geol*, 634, <https://doi.org/10.1016/j.chemgeo.2023.121572>,
463 2023.

464

465 Suh, Y. J., Diefendorf, A. F., Bowen, G. J., Cotton, J. M., and Ju, S. J.: Plant wax integration and
466 transport from the Mississippi River Basin to the Gulf of Mexico inferred from GIS-
467 enabled isoscapes and mixing models, *Geochim Cosmochim Acta*, 257, 131–149,
468 <https://doi.org/10.1016/j.gca.2019.04.022>, 2019.

469

470 Tornero, C., Balasse, M., Bălăşescu, A., Chataigner, C., Gasparyan, B., and Montoya, C.: The
471 altitudinal mobility of wild sheep at the Epigravettian site of Kalavan 1 (Lesser Caucasus,
472 Armenia): Evidence from a sequential isotopic analysis in tooth enamel, *J Hum Evol*, 97,
473 27–36, <https://doi.org/10.1016/j.jhevol.2016.05.001>, 2016b.

474

475 Trigui, Y., Wolf, D., Sahakyan, L., Hovakimyan, H., Sahakyan, K., Zech, R., Fuchs, M.,
476 Wolpert, T., Zech, M., and Faust, D.: First calibration and application of leaf wax n-
477 alkane biomarkers in loess-paleosol sequences and modern plants and soils in Armenia,
478 *Geosciences (Switzerland)*, 9, <https://doi.org/10.3390/geosciences9060263>, 2019.

479

480

481 Volodicheva, N.: The Caucasus, The physical geography of northern Eurasia, 350–376, 2002.

482

483

484

485

486

487

488

489

490

491

492

	Conc¹	NPP²	ACL³	$\delta^{13}\text{C}^3$	δD^3
Forest	7.69	1099.4	29.5	-33.3	-156
Alpine Meadow	3.03	719.1	30.6	-34.9	-175

Table 1: Constants used for mixing model. 1: *n*-alkane concentration in grasses and trees in the Caucasus Mountains (grams of *n*-alkane/gram of organic material) (Bliedtner et al., 2018; Trigui et al., 2019). 2: NPP for forest and grassland areas (grams per area) (Brun et al., 2022). 3: mean values for ACL, $\delta^{13}\text{C}$ and δD (this study)

494 Figure Captions

495 Figure 1: (Left) Topographic map (ASTER Global DEM) of Armenia with inset map of
496 sampling location (black box) (Right) Inset map of soil (yellow circles) and stream (blue circles)
497 samples collected in the Areguni Mountains, along with the limit of the Barepat (dashed line)
498 and Dany watersheds (solid line)

499 Figure 2: The δD and $\delta^{13}C$ values of *n*-alkanes extracted from above treeline (green squares) and
500 below treeline (red triangles) sediments

501 Figure 3: The average chain length (ACL) values of *n*-alkanes extracted from above treeline
502 (yellow squares) and below treeline (green squares) sediment across the sampling elevation
503 gradient

504 Figure 4: The $\delta^{13}C$ values of *n*-alkanes extracted from above treeline (yellow squares) and below
505 treeline (green squares) sediment across the sampling elevation gradient

506 Figure 5: The δD values of *n*-alkanes extracted from above treeline (yellow squares) and below
507 treeline (green squares) sediment across the sampling elevation gradient

508 Figure 6: Mixing model used to calculate expected values of stream sample points. Upstream
509 watershed area covered by deciduous forest (green) and alpine meadow (yellow) was calculated
510 at each sample location (blue dots). Point watershed for sample 24 (dashed line) is shown here as
511 an example.

512 Figure 7: Comparison of the measured ACL, δD and $\delta^{13}C$ values against expected values of
513 stream sediments. Dashed line represents the range of expected values from stream sediments if
514 vegetation was integrated equally by area

515 Figure 8: A photograph of the Dany watershed with hypothetical paleoclimate record from three
516 locations: (A, dashed line) Below treeline, (B, solid line) near treeline with fluctuations in
517 treeline altitude, and (C, dotted line) above treeline

518

519

520

521

522

523

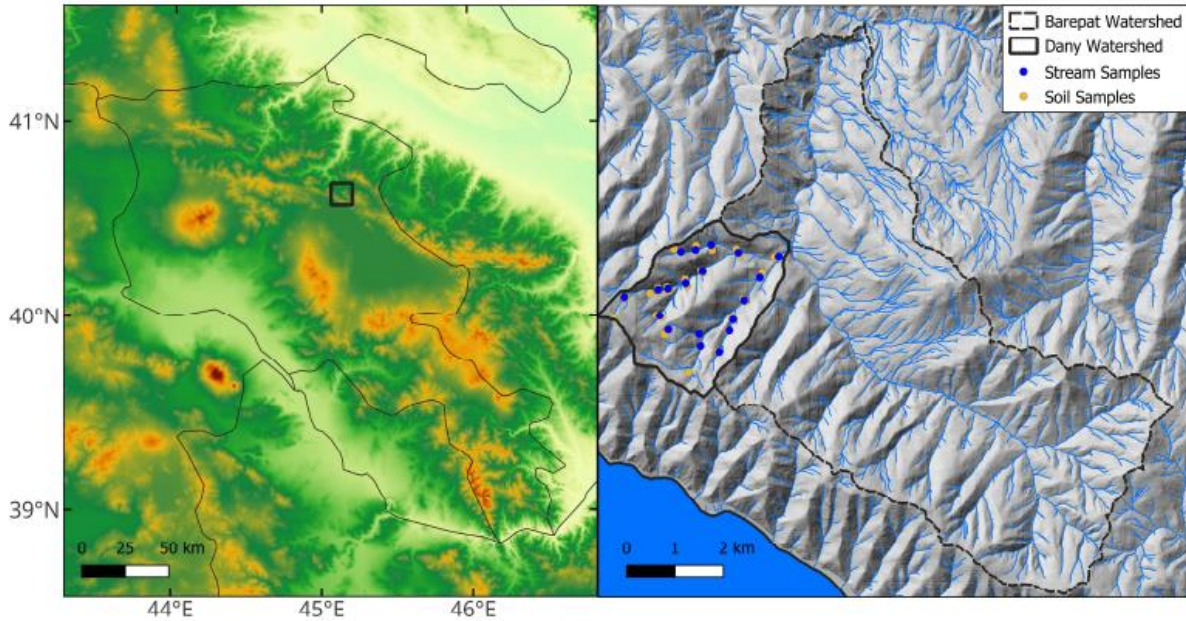


Figure 1: (Left) Topographic map (ASTER Global DEM) of Armenia with inset map of sampling location (black box) (Right) Inset map of soil (yellow circles) and stream (blue circles) samples collected in the Areguni Mountains, along with the limit of the Barepat (dashed line) and Dany watersheds (solid line)

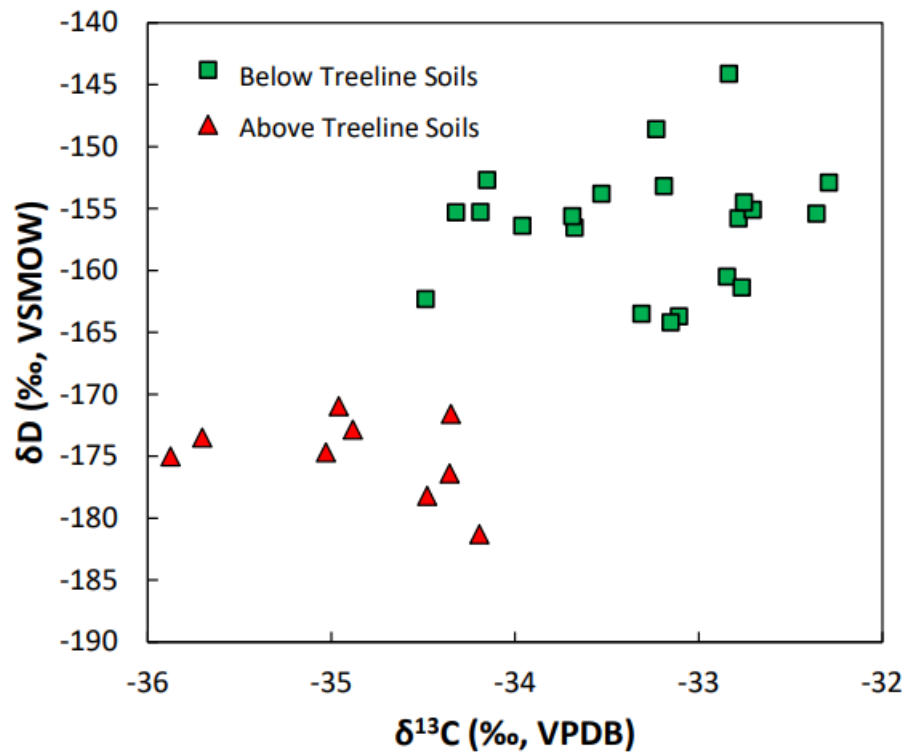


Figure 2: The δD and $\delta^{13}\text{C}$ values of *n*-alkanes extracted from above treeline (green squares) and below treeline (red triangles) sediments

525
526
527
528
529
530
531
532
533
534
535
536
537
538
539
540
541
542
543
544

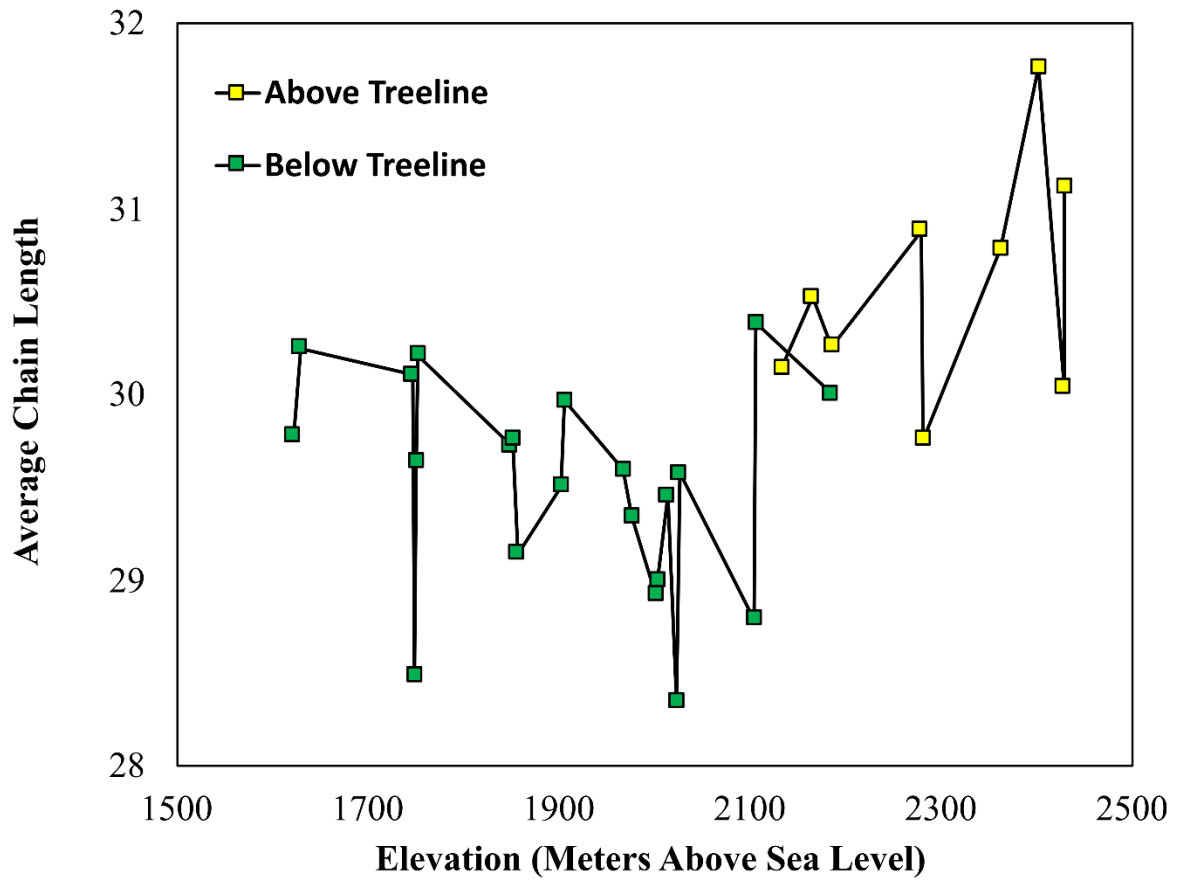


Figure 3: The average chain length (ACL) values of *n*-alkanes extracted from above treeline (yellow squares) and below treeline (green squares) sediment across the sampling elevation gradient

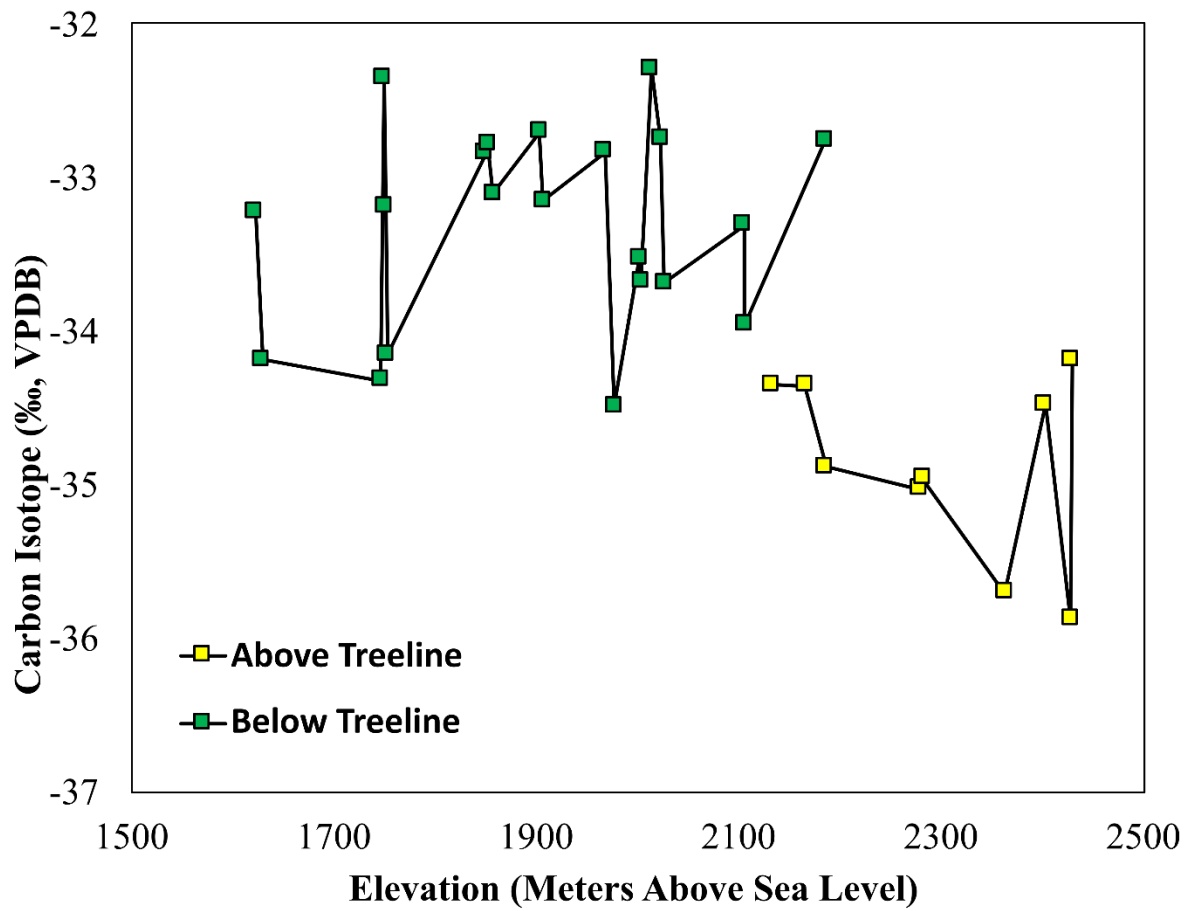


Figure 4: The $\delta^{13}\text{C}$ values of *n*-alkanes extracted from above treeline (yellow squares) and below treeline (green squares) sediment across the sampling elevation gradient

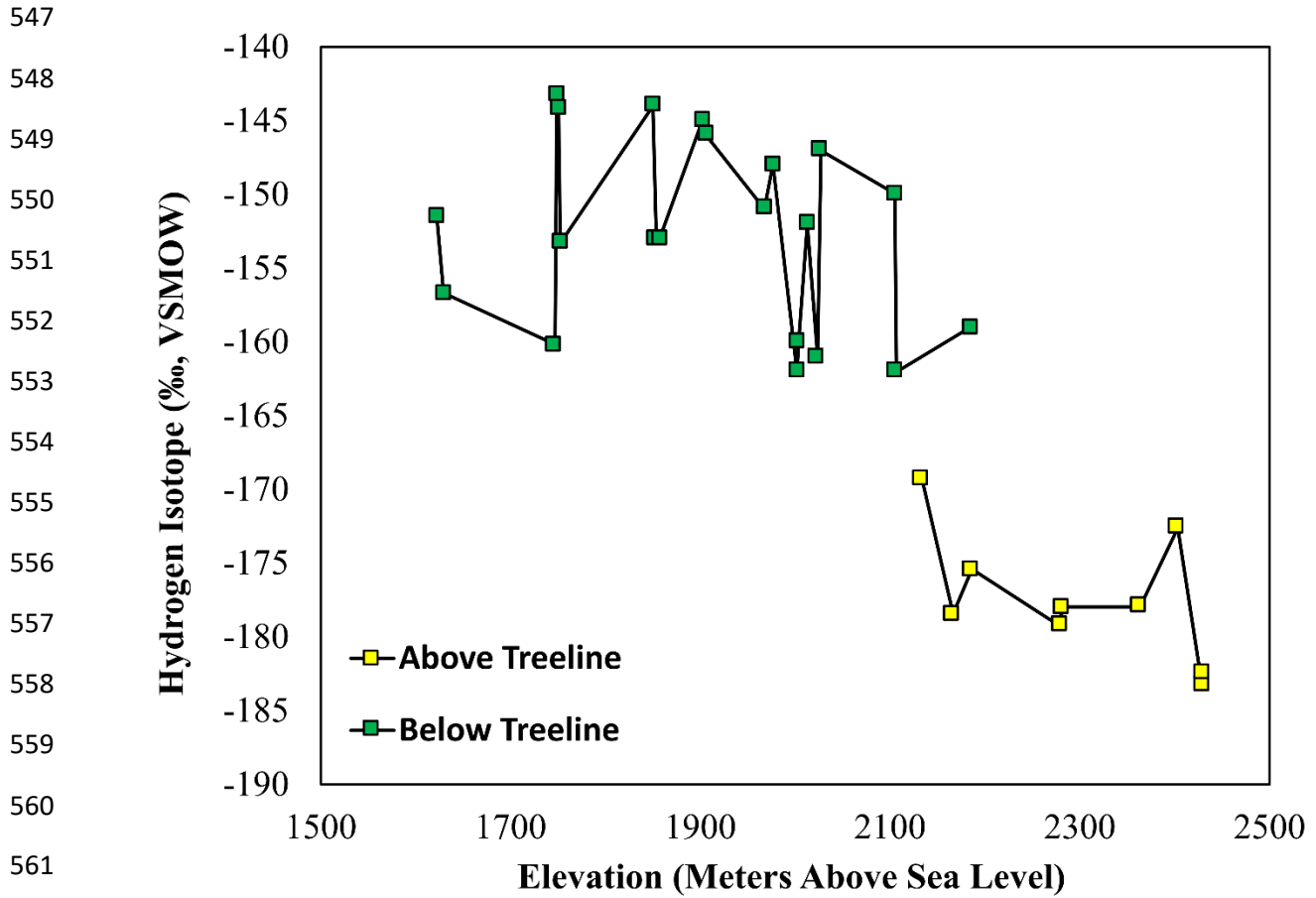


Figure 5: The δD values of *n*-alkanes extracted from above treeline (yellow squares) and below treeline (green squares) sediment across the sampling elevation gradient

567
568
569

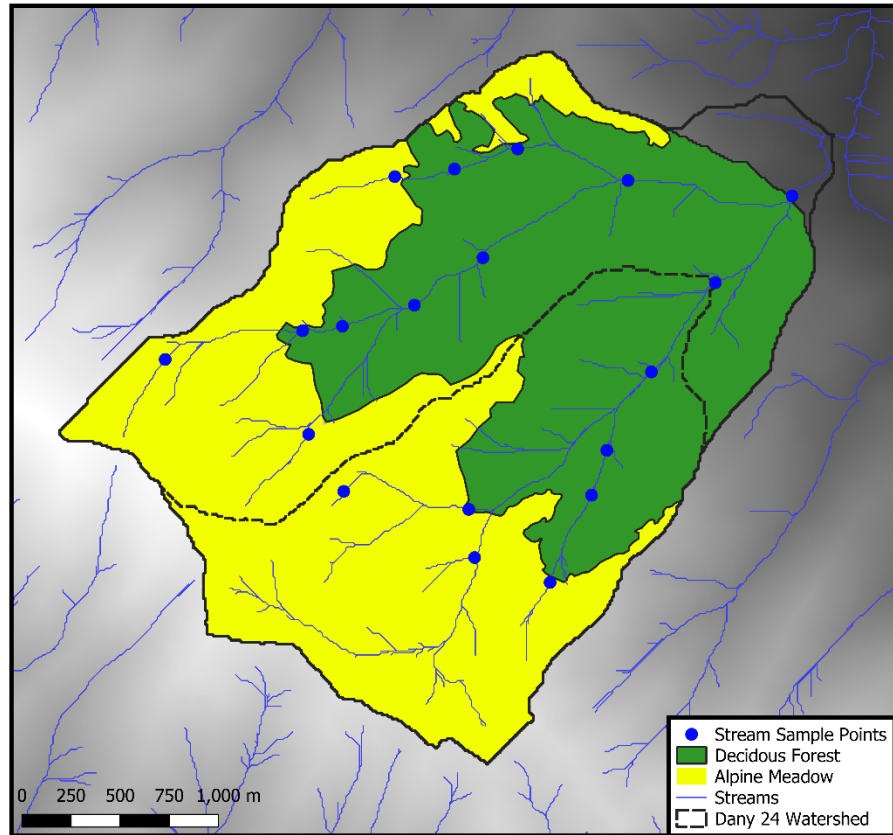


Figure 6: Mixing model used to calculate expected values of stream sample points. Upstream watershed area covered by deciduous forest (green) and alpine meadow (yellow) was calculated at each sample location (blue dots). Point watershed for sample 24 (dashed line) is shown here as an example.

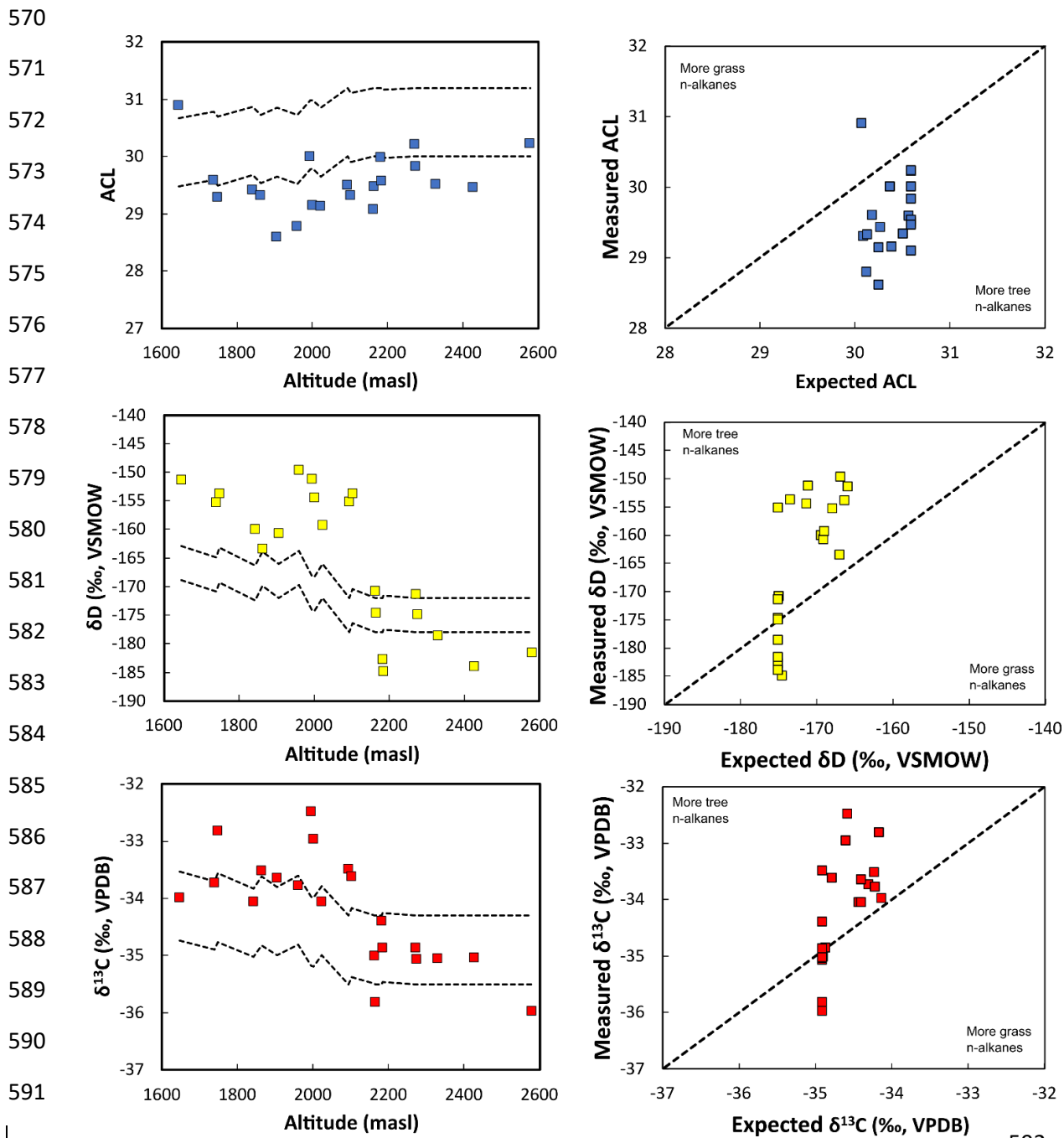


Figure 7: Comparison of the measured ACL, δD and $\delta^{13}C$ values against expected values of stream sediments. Dashed line represents the range of expected values from stream sediments if vegetation was integrated equally by area

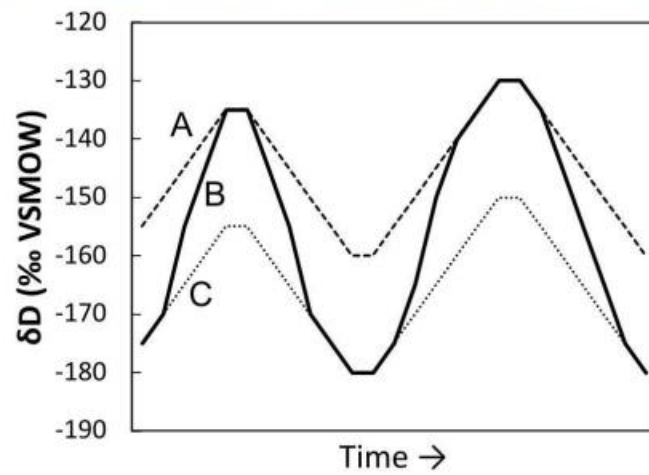
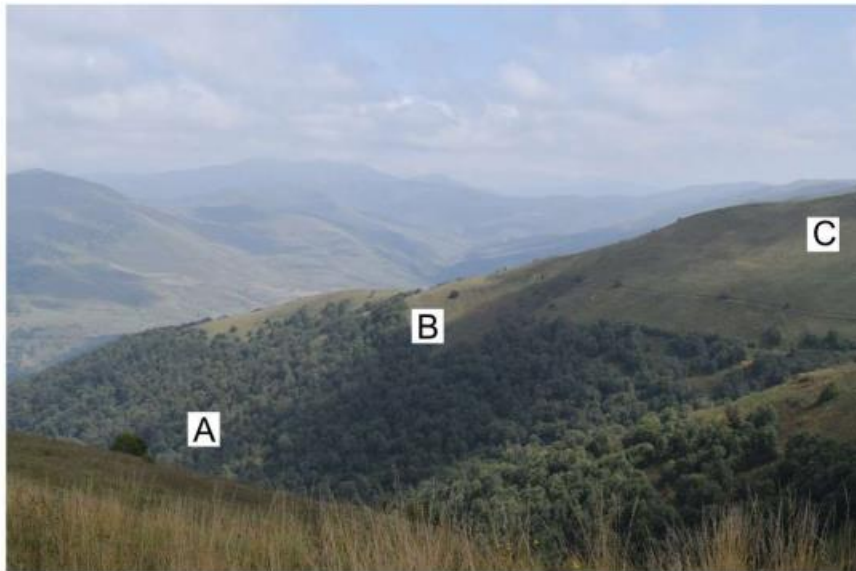


Figure 8: A photograph of the Dany watershed with hypothetical paleoclimate record from three locations: (A, dashed line) Below treeline, (B, solid line) near treeline with fluctuations in treeline altitude, and (C, dotted line) above treeline